Electronic Supplementary Material (ESI) for Catalysis Science & Technology.

Enhancing bimetallic synergy with light: The effect of UV light pre-treatment on catalytic oxygen activation by bimetallic Au-Pt nanoparticles on a TiO_2 support

Roong Jien Wong[†], *Jason Scott*[†*], *Peter Kappen*[‡], *Gary K.-C. Low*[†], *Judy N. Hart*[§], *Rose Amal*[†*]

[†]Particles and Catalysis Research Group, School of Chemical Engineering, The University of New South Wales, Sydney, NSW 2052, Australia.

[‡]Australian Synchrotron, 800 Blackburn Road, Clayton, Victoria 3168, Australia.

[§]School of Materials Science and Engineering, The University of New South Wales, Sydney, NSW 2052, Australia.

*E-mail: jason.scott@unsw.edu.au, r.amal@unsw.edu.au

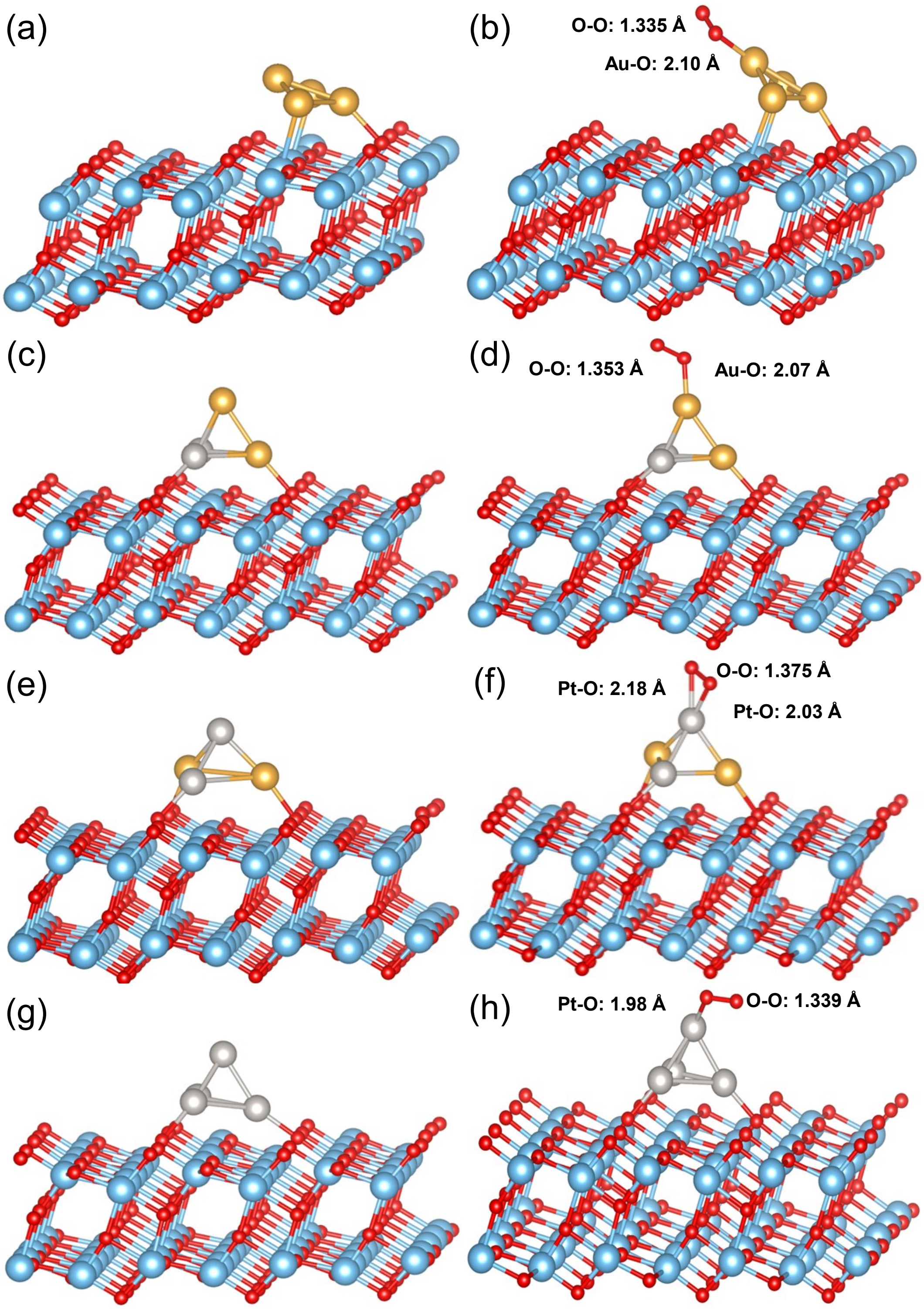

Figure S1. Optimised TiO_2 slab models used for DFT calculations for (a) Au_4/TiO_2, (c) Au_2Pt_2/TiO_2 (Au on top), (e) Au_2Pt_2/TiO_2 (Pt on top), and (g) Pt_4/TiO_2, and (b, d, f, h) their respective models with O_2 molecules adsorbed.

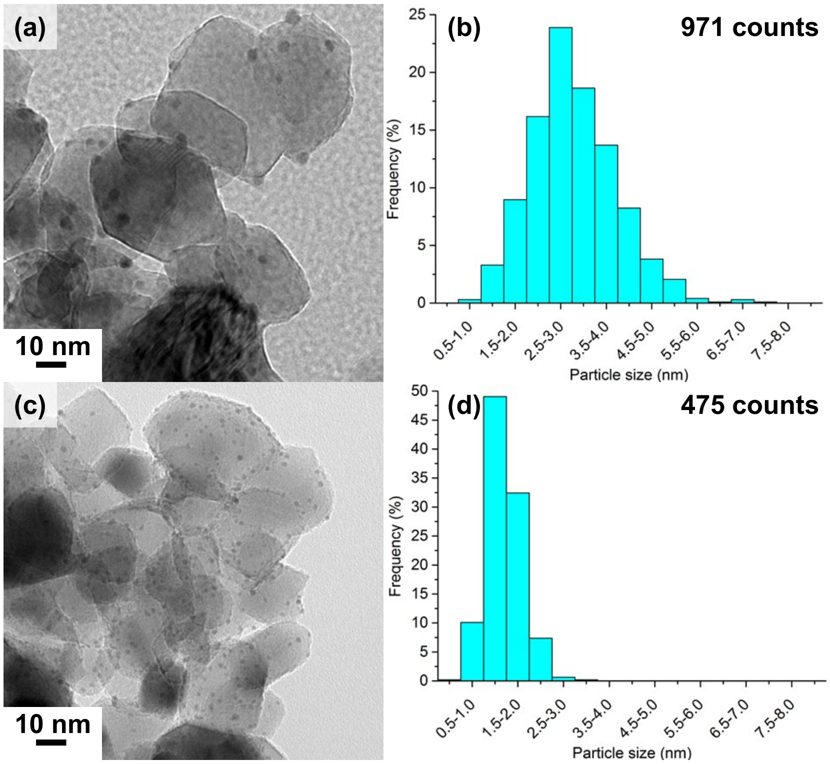

Figure S2. Representative TEM images of (a) Au/TiO_2 and (c) Pt/TiO_2, and their respective particle size distributions (b and d).

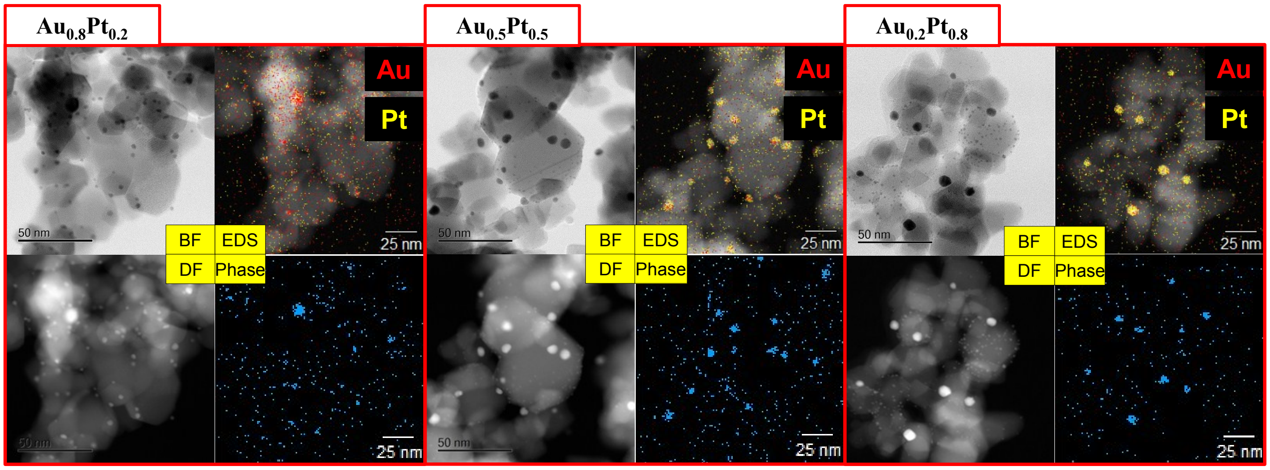

Figure S3. STEM imaging in bright field mode (BF), dark field mode (DF), EDS mapping, and phase mapping (Phase) of (*from left to right*) $Au_{0.8}Pt_{0.2}/TiO_2$, $Au_{0.5}Pt_{0.5}/TiO_2$, and $Au_{0.2}Pt_{0.8}/TiO_2$, respectively.

EDS and phase mappings show that the $Au_{0.8}Pt_{0.2}/TiO_2$ has bimetallic alloy nanoparticles throughout the sample, while the excess Pt in $Au_{0.5}Pt_{0.5}/TiO_2$ and $Au_{0.2}Pt_{0.8}/TiO_2$ forms small Pt nanoparticles.

Table S1. ICP-OES analysis revealing the Au and Pt loadings on the bimetallic AuxPty/TiO2 catalysts.

Sample	Au (at%)	Pt (at%)	Au:Pt ratio
$Au_{0.8}Pt_{0.2}/TiO_2$	0.46	0.11	4.18
$Au_{0.5}Pt_{0.5}/TiO_2$	0.49	0.28	1.75
$Au_{0.2}Pt_{0.8}/TiO_2$	0.12	0.57	0.21

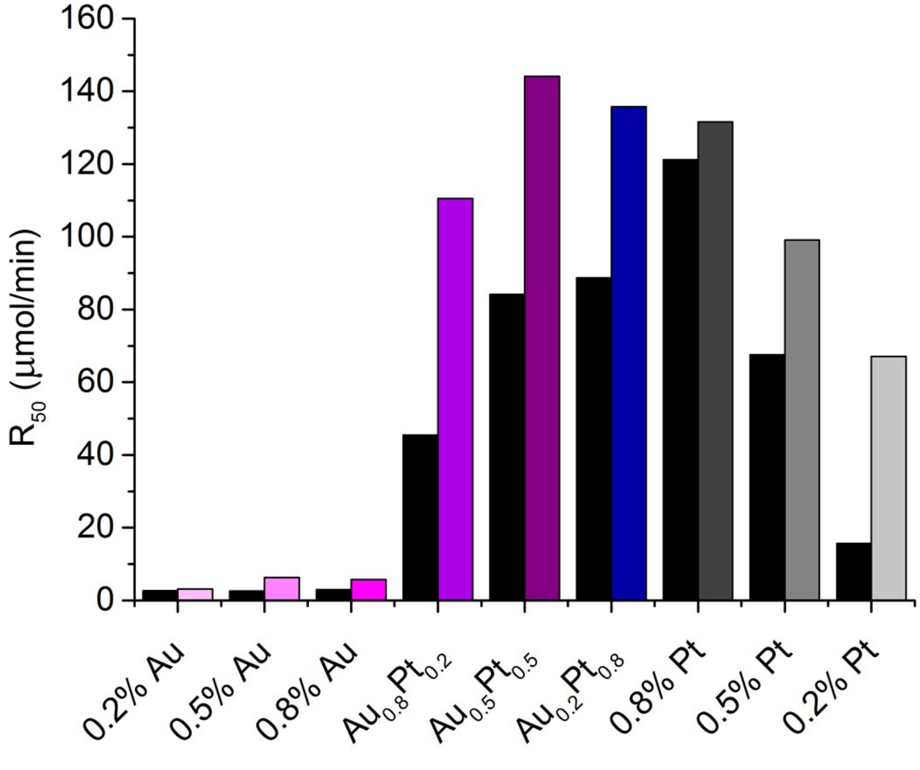

Figure S4. Rate at which 50 % of the initial formic acid added is oxidised (R_{50}) for Au/TiO_2, Pt/TiO_2, and $AuPt/TiO_2$ at various metal loadings, with (coloured columns) and without (black columns) UV pre-illumination. Pre-illumination time: 30 min; total formic acid loading: 1000 μmol. Pink columns represent Au/TiO_2; grey columns represent Pt/TiO_2; colour tones indicate the relative metal loadings of Au and Pt.

Comparing the R_{50} values of the bimetallic Au-Pt/TiO_2 catalysts with the monometallic Au/TiO_2 and Pt/TiO_2 catalysts highlights the bimetallic synergy effect. The improvement in activity cannot be solely attributed to the presence of small Pt nanoparticles in the bimetallic catalysts (Figure 1, main text), as the monometallic Pt/TiO_2 catalysts with corresponding Pt loadings yield significantly different R_{50} values.

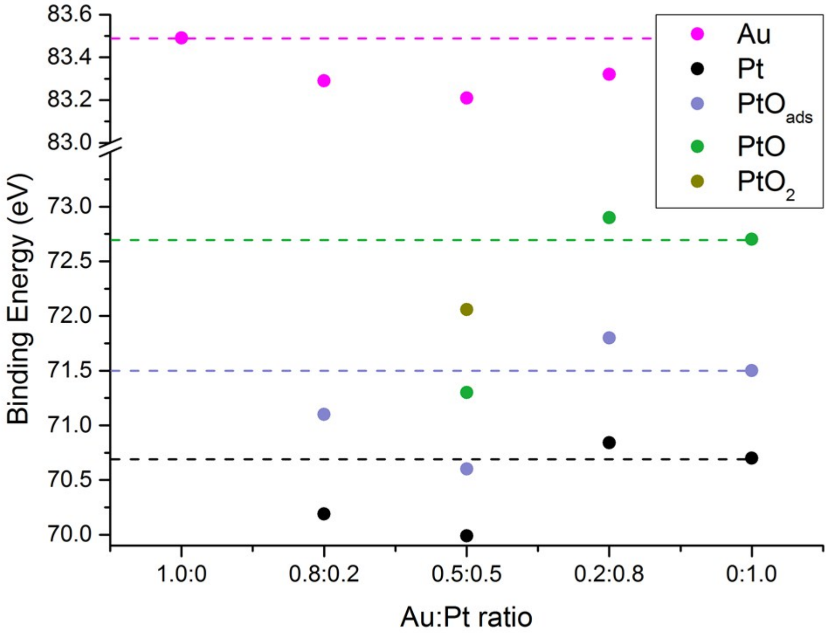

Figure S5. Au4f and Pt4f binding energies of AuPt/TiO_2 with various Au:Pt ratios. The horizontal dotted lines indicate the binding energies of Au and Pt species for the monometallic nanoparticles supported on TiO_2.

The shifts in binding energies and the Pt speciation of bimetallic AuPt/TiO_2 suggest the bimetallic catalyst behaviour resembles the monometallic Pt/TiO_2 at high Pt loading, due to the inhomogeneity of Au-Pt bimetallic alloy structure. Pt speciation of $Au_{0.2}Pt_{0.8}$/TiO_2 shows the presence of PtO species, similar to monometallic Pt/TiO_2, without a gain in electron density. The formation of PtO creates a metal oxide phase in the Au-Pt bimetallic alloy, causing the Au-Pt phase segregation. This indicates the Au-Pt bimetallic interaction is weaker in $Au_{0.2}Pt_{0.8}/TiO_2$ relative to the other two bimetallic catalysts. The presence of PtO, which appears at the nanoscale, is not taken into account in the bulk Au-Pt phase diagram and introduces a slight inconsistency within the bulk material miscibility data.

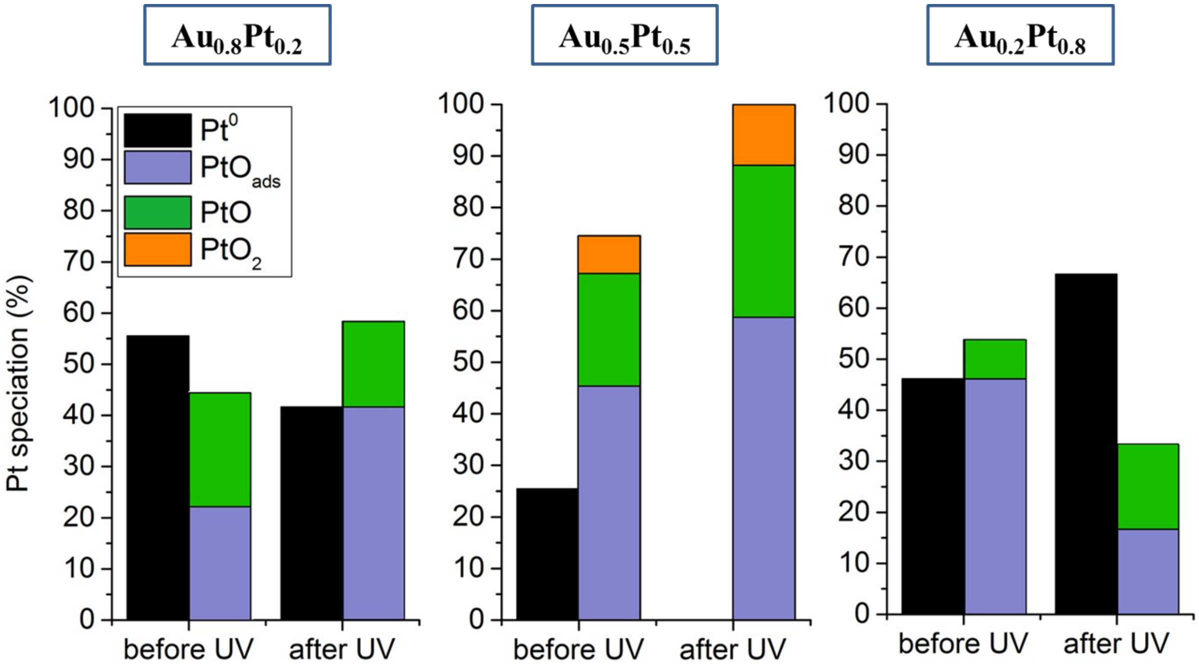

Figure S6. Pt speciation before and after UV light pre-treatment. Pre-illumination enhancement is related to the percentage of Pt interacting with O to form active oxygen species after UV light pre-treatment.

Pt speciation of AuPt/TiO_2 catalysts before and after pre-illumination shows an increase in active oxygen content for $Au_{0.8}Pt_{0.2}/TiO_2$ and $Au_{0.5}Pt_{0.5}/TiO_2$, but not as much for $Au_{0.2}Pt_{0.8}/TiO_2$. The presence of PtO_2 species in $Au_{0.5}Pt_{0.5}/TiO_2$ indicates the bimetallic catalyst is capable of activating more oxygen for formic acid oxidation, which can be seen from its higher overall oxidation rate. The decrease in PtO_{ads} with the increase in PtO in $Au_{0.2}Pt_{0.8}/TiO_2$ is supportive of the Au-Pt surface segregation, which leads to a decrease in catalytic oxygen activation.

Table S2. Mulliken charges of the Au and Pt atoms on TiO_2 support at various bimetallic alloying ratios.

Metal cluster	**Mulliken charges**
Au	-0.13 (-0.16), -0.13 (-0.15), +0.36 (+0.35), +0.20* (+0.01*)
Au_2Pt_2 (Au on top)	Au: +0.44 (+0.43), +0.21* (+0.04*) Pt: -0.15 (-0.17), -0.14 (-0.17)
Au_2Pt_2 (Pt on top)	Au: +0.39 (+0.37), +0.42 (+0.41) Pt: -0.16 (-0.19), -0.22* (-0.37*)
Pt	+0.04 (-0.08), +0.04 (-0.08), -0.02 (-0.11), +0.08* (-0.09*)

Note: Values in parentheses indicate the resulting Mulliken charges of atoms upon introducing an extra electron into the simulation cell, simulating the effect of UV light pre-treatment. * indicates the atom at the top of the cluster at which O_2 molecule is bonded to in the DFT calculations (refer to Table 1 in main text).

An overall increase in electron density (Mulliken charges) was observed in the Pt for all three bimetallic samples, with an overall decrease in the Au, supporting the claim that electrons are transferred from Au to Pt. The decrease in electron density of Au in Au/TiO_2 is attributed to the delocalisation of electrons at the metal-support interface, which becomes apparent due to the small bimetallic clusters used in the calculations[1]. However, the net charge increase in the metal clusters observed from the XPS was not predicted by the DFT calculation, most likely due to the smaller cluster size compared with the experiments and the fact that the difference in cluster size was not considered in the DFT calculations. It has been reported that work function, the proposed driving force for electron transfer, is a function of particle size and charge[2]. Larger particles have higher work function. As seen from the STEM images, $Au_{0.5}Pt_{0.5}/TiO_2$ has larger bimetallic alloy particles than $Au_{0.8}Pt_{0.2}/TiO_2$, suggesting the $Au_{0.5}Pt_{0.5}$ bimetallic alloy particles have higher work function. The higher work function is expected to cause the greater net charge transfer, which is consistent with the XPS observations. UV light pre-treatment, simulated by introducing an extra electron into the simulation cell, increases the electron density of the metal clusters, especially the Pt sites. The change in electron densities highlights the electron flow due to UV light pre-treatment and O_2 adsorption.

Table S3. Structural parameters of bulk metals and catalysts as determined in the first-shell EXAFS analyses.

Catalyst	Condition	shell	N	$\Delta\sigma^2$ (10^{-3} Å^2)	R (Å)	ΔE_0 (eV)
Au foil[a]		Au-Au	12	0	2.85	0
Pt foil[a]		Pt-Pt	12	0	2.76	0
0.8 at% Au/TiO_2	Dark	Au-Au	7.5 ± 0.5	2.4 ± 0.6	2.85 ± 0.00	6.5 ± 0.6
0.2 at% Pt/TiO_2	Dark	Pt-Pt	10.4 ± 5.1	18.5 ± 5.4	2.57 ± 0.03	-5.1 ± 3.7
		Pt-O	1.8 ± 1.1		1.95 ± 0.04	
$Au_{0.8}Pt_{0.2}/TiO_2$	Dark	Au-M[b]	10.4 ± 0.7	4.2 ± 0.2	2.84 ± 0.00	7.6 ± 0.8
		Pt-M	7.3 ± 1.5	4.9 ± 2.2	2.76 ± 0.02	8.1 ± 2.3
		Pt-O	0.5 ± 0.3		1.85 ± 0.05	
	UV	Au-M	10.3 ± 0.7	4.1 ± 0.3	2.85 ± 0.00	7.9 ± 0.9
		Pt-M	6.9 ± 1.2	3.8 ± 1.9	2.76 ± 0.02	8.6 ± 2.0
		Pt-O	0.7 ± 0.3		2.05 ± 0.04	
$Au_{0.5}Pt_{0.5}/TiO_2$	Dark	Au-M	11.8 ± 1.0	3.6 ± 0.3	2.85 ± 0.0	7.7 ± 1.1
		Pt-M	6.3 ± 1.0	4.4 ± 1.8	2.74 ± 0.02	8.1 ± 2.3
		Pt-O	1.4 ± 0.3		2.07 ± 0.02	
$Au_{0.2}Pt_{0.8}/TiO_2$	Dark	Au-M	N.D.	N.D.	N.D.	N.D.
		Pt-M	5.3 ± 0.6	2.3 ± 1.1	2.71 ± 0.01	7.4 ± 1.3
		Pt-O	0.8 ± 0.2		2.01 ± 0.02	
	UV	Au-M	N.D.	N.D.	N.D.	N.D.
		Pt-M	5.8 ± 0.8	3.7 ± 1.5	2.69 ± 0.01	5.2 ± 1.8
		Pt-O	1.7 ± 0.3		2.03 ± 0.01	

Dark: without UV light pre-treatment; UV: after 30 min UV light pre-treatment; N.D.: not determined; a: extracted from Bus and Bokhoven[3]; b: M = Au or Pt.

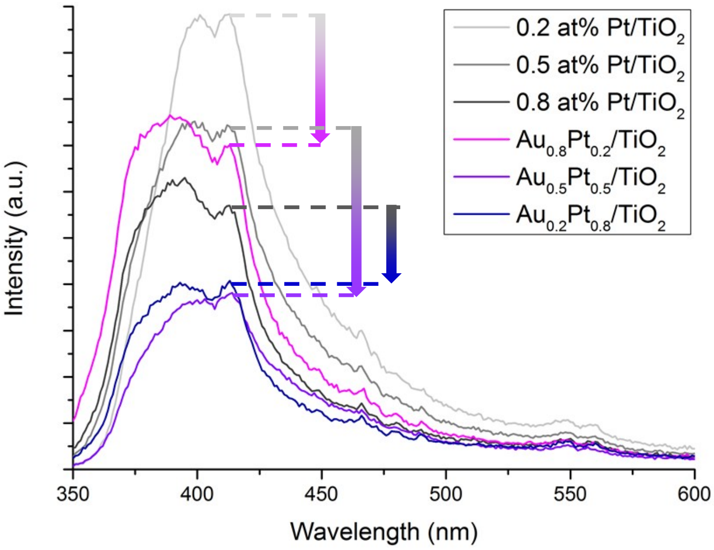

Figure S7. PL measurements illustrate the decrease in recombination rate of AuPt/TiO_2 compared to Pt/TiO_2 of various loadings, consistent with the notion of Au acting as the electron reservoir for Pt in the bimetallic catalysts.

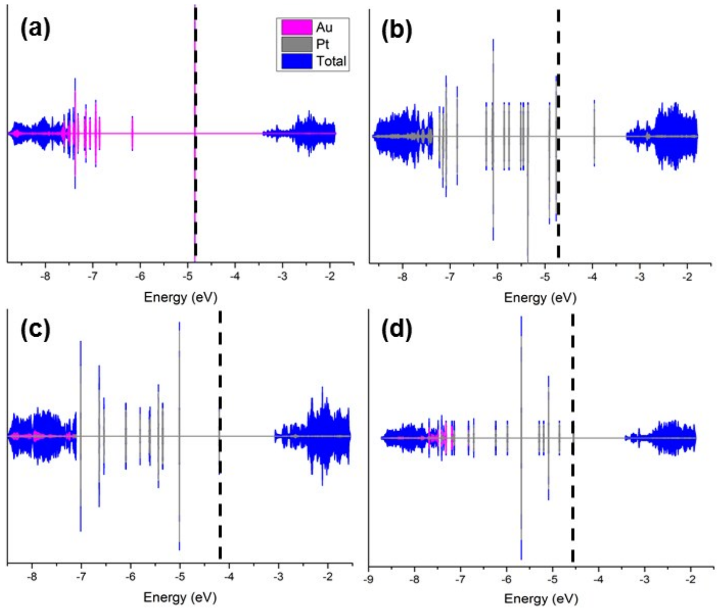

Figure S8. Density of states of: (a) Au/TiO_2, (b) Pt/TiO_2, (c) Au_2Pt_2/TiO_2 (Au on top), and (d) Au_2Pt_2/TiO_2 (Pt on top) obtained from DFT calculations. The black dotted lines indicate the maximum occupied energy states in the ground state.

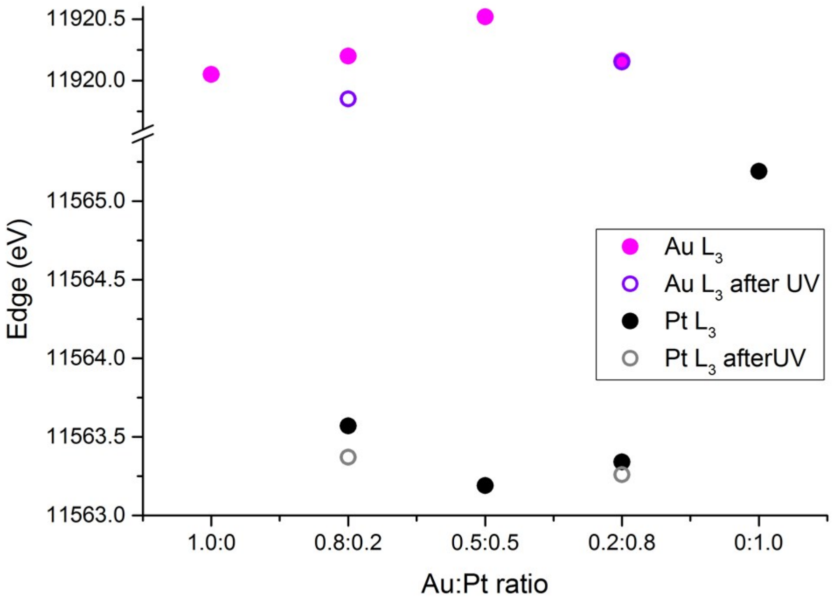

Figure S9. Effect of UV light pre-treatment on the Au L_3 and Pt L_3 absorption edges at various Au:Pt ratio.

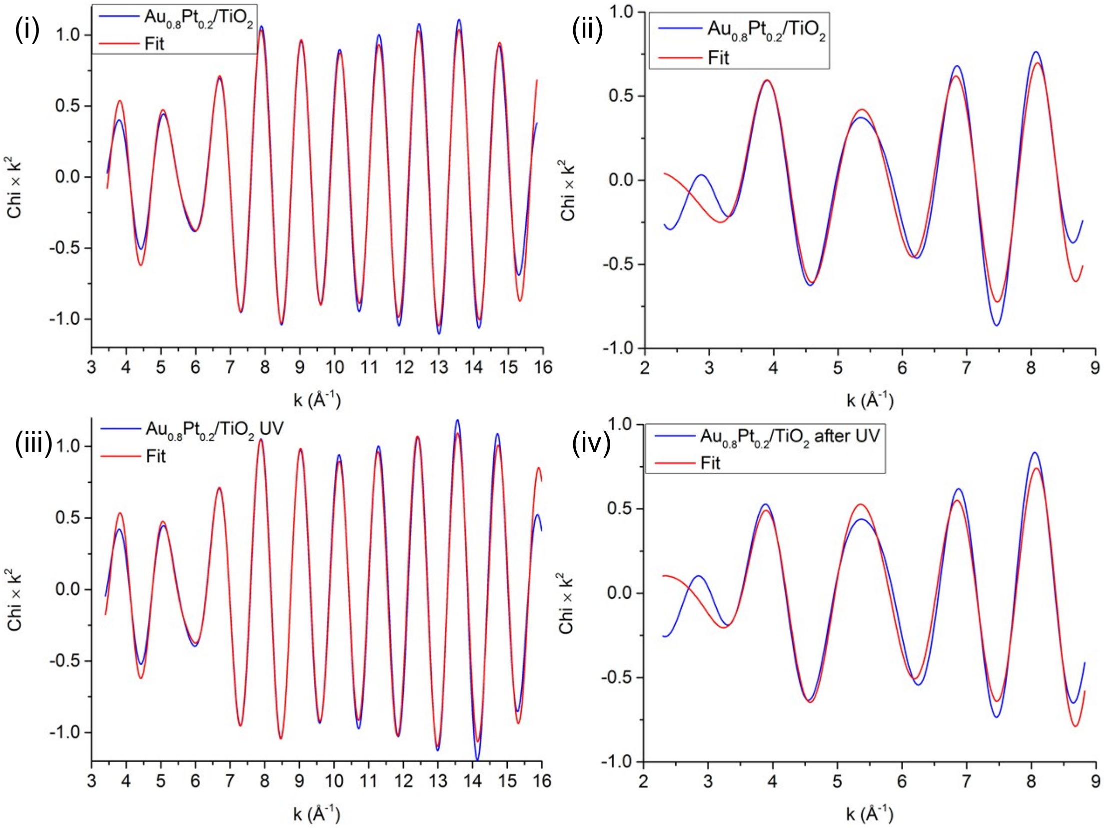

Figure S10. EXAFS fit of $Au_{0.8}Pt_{0.2}/TiO_2$ at the Au L_3 (i, iii) and Pt L_3 (ii, iv) edges, before and after UV light pre-treatment in Back Fourier Transformed k-space.

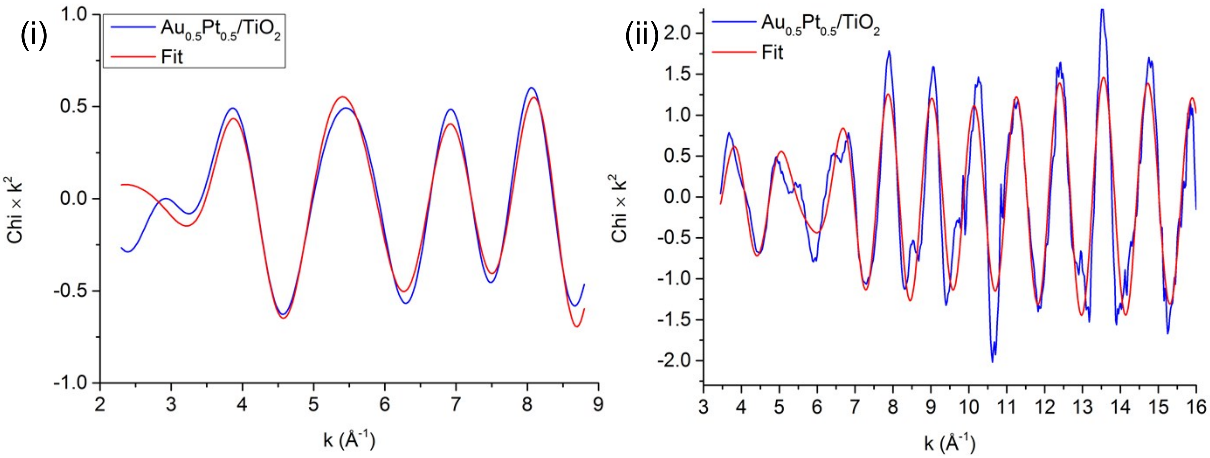

Figure S11. EXAFS fit of $Au_{0.5}Pt_{0.5}/TiO_2$ at the Au L_3 (i) and Pt L_3 (ii) edges without UV light pre-treatment in Back Fourier Transformed k-space.

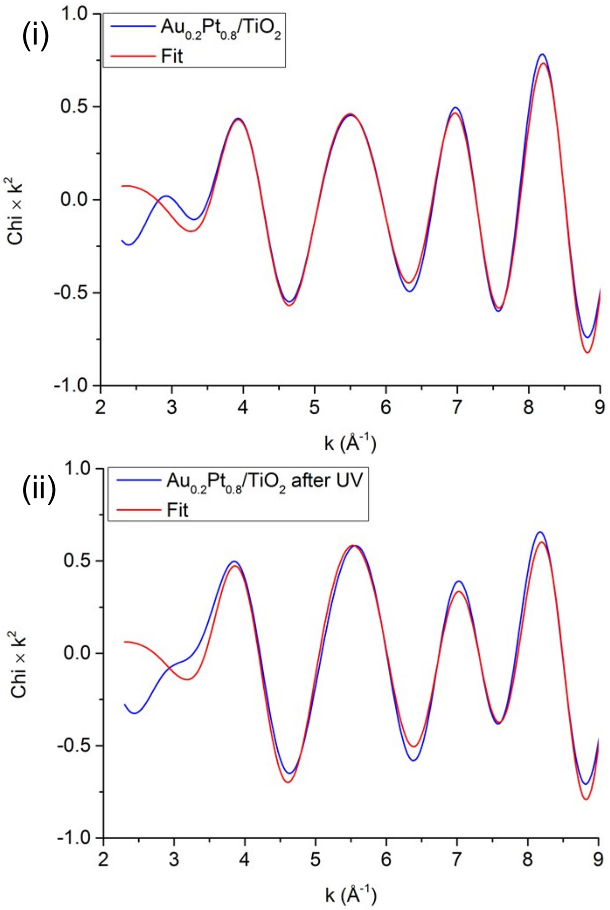

Figure S12. EXAFS fit of $Au_{0.2}Pt_{0.8}/TiO_2$ at the Pt L_3 edge before (i) and after (ii) UV light pre-treatment in Back Fourier Transformed k-space.

EXAFS fittings were performed taking into consideration the overlapping of Au L_3 edge in the Pt L_3 edge at high k values. The main aim of EXAFS fittings is to determine the change in the Au and Pt interatomic distances.

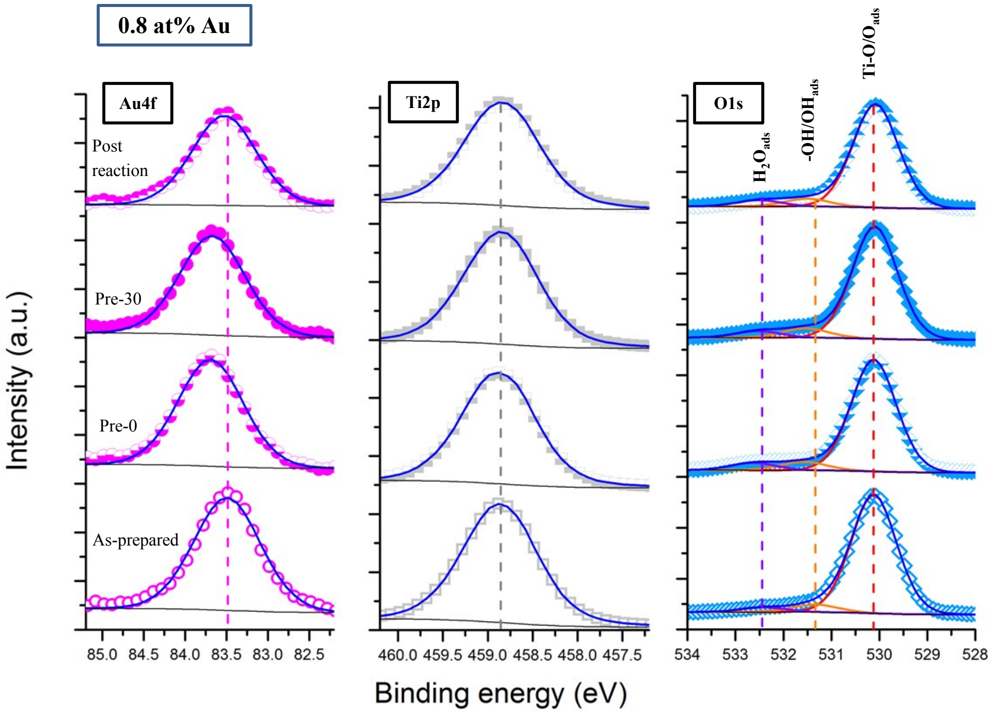

Figure S13. XPS Au4f, Ti2p, and O1s spectra of 0.8 at% Au/TiO$_2$ at the as-prepared state, before UV light pre-treatment (Pre-0), after 30 min UV light pre-treatment (Pre-30), and post-reaction.

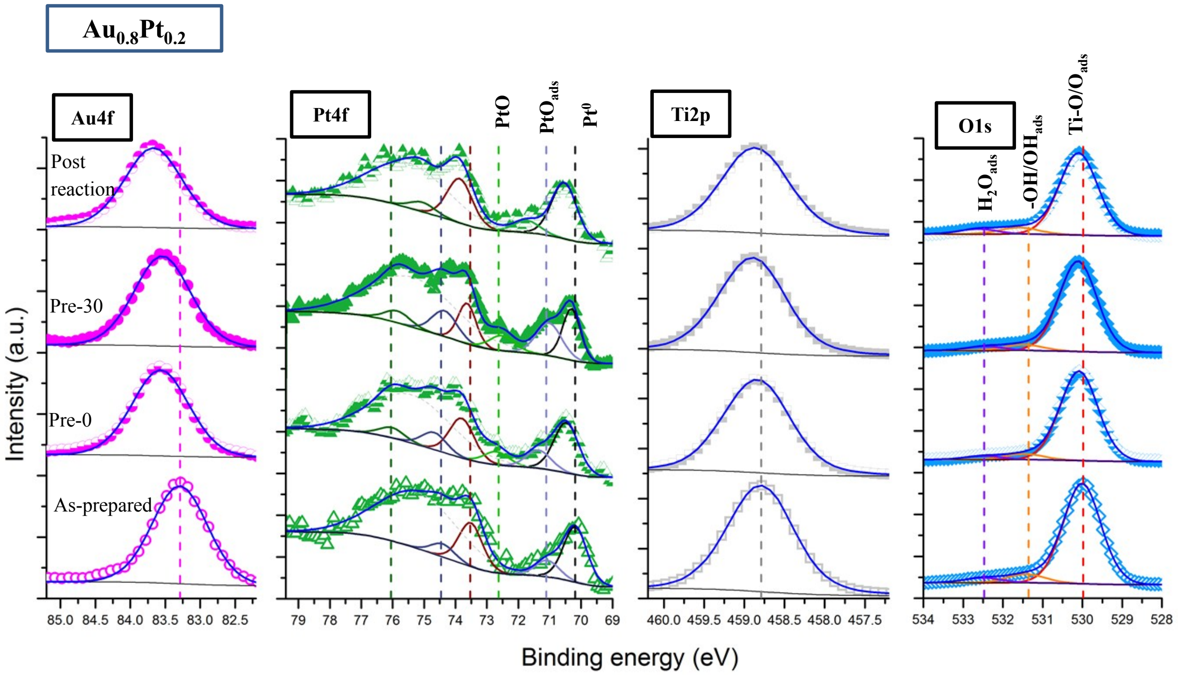

Figure S14. XPS Au4f, Pt4f, Ti2p, and O1s spectra of $Au_{0.8}Pt_{0.2}/TiO_2$ at the as-prepared state, before UV light pre-treatment (Pre-0), after 30 min UV light pre-treatment (Pre-30), and post-reaction.

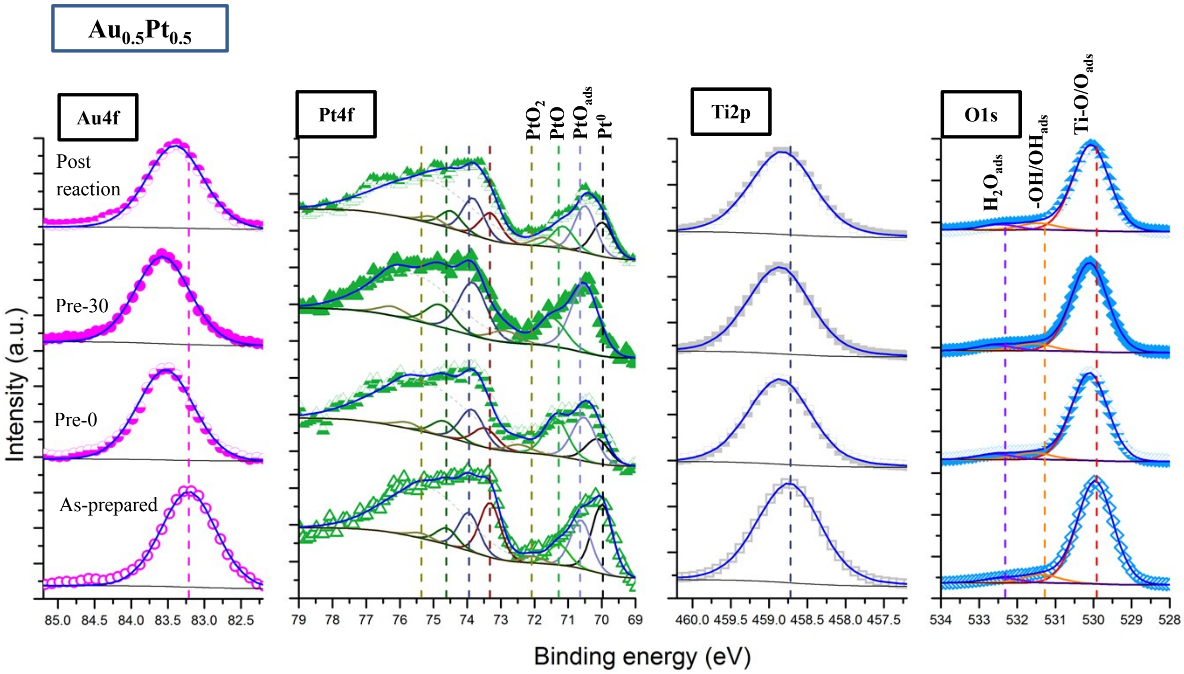

Figure S15. XPS Au4f, Pt4f, Ti2p, and O1s spectra of $Au_{0.5}Pt_{0.5}/TiO_2$ at the as-prepared state, before UV light pre-treatment (Pre-0), after 30 min UV light pre-treatment (Pre-30), and post-reaction.

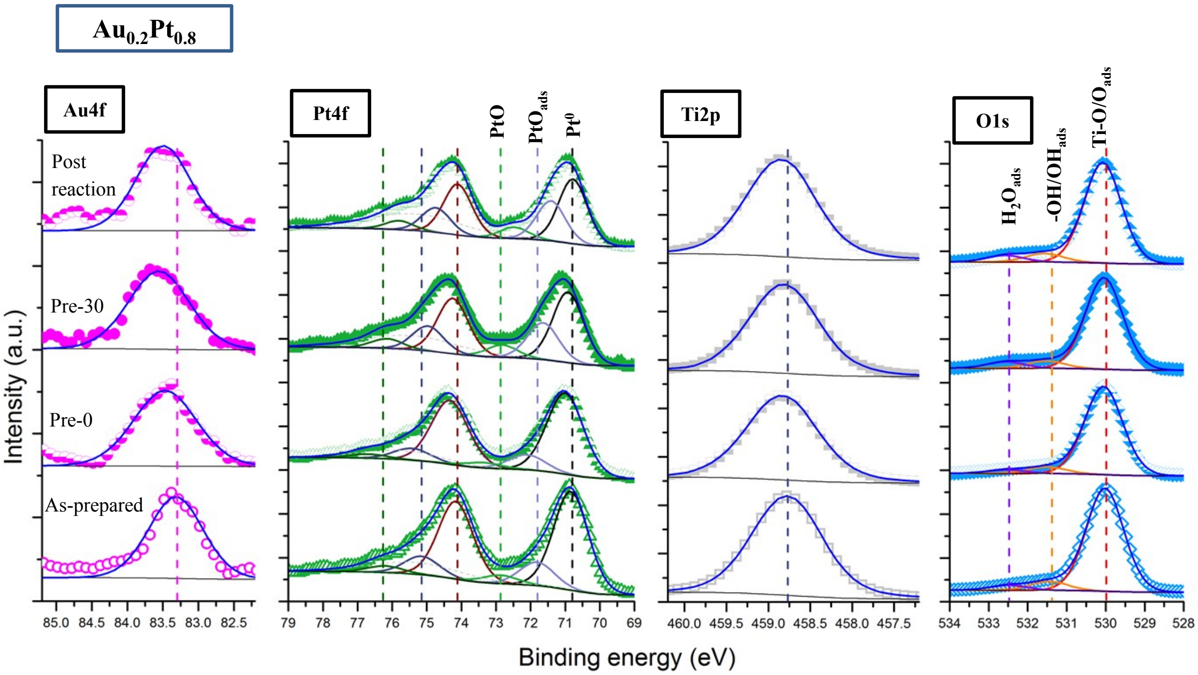

Figure S16. XPS Au4f, Pt4f, Ti2p, and O1s spectra of $Au_{0.2}Pt_{0.8}/TiO_2$ at the as-prepared state, before UV light pre-treatment (Pre-0), after 30 min UV light pre-treatment (Pre-30), and post-reaction.

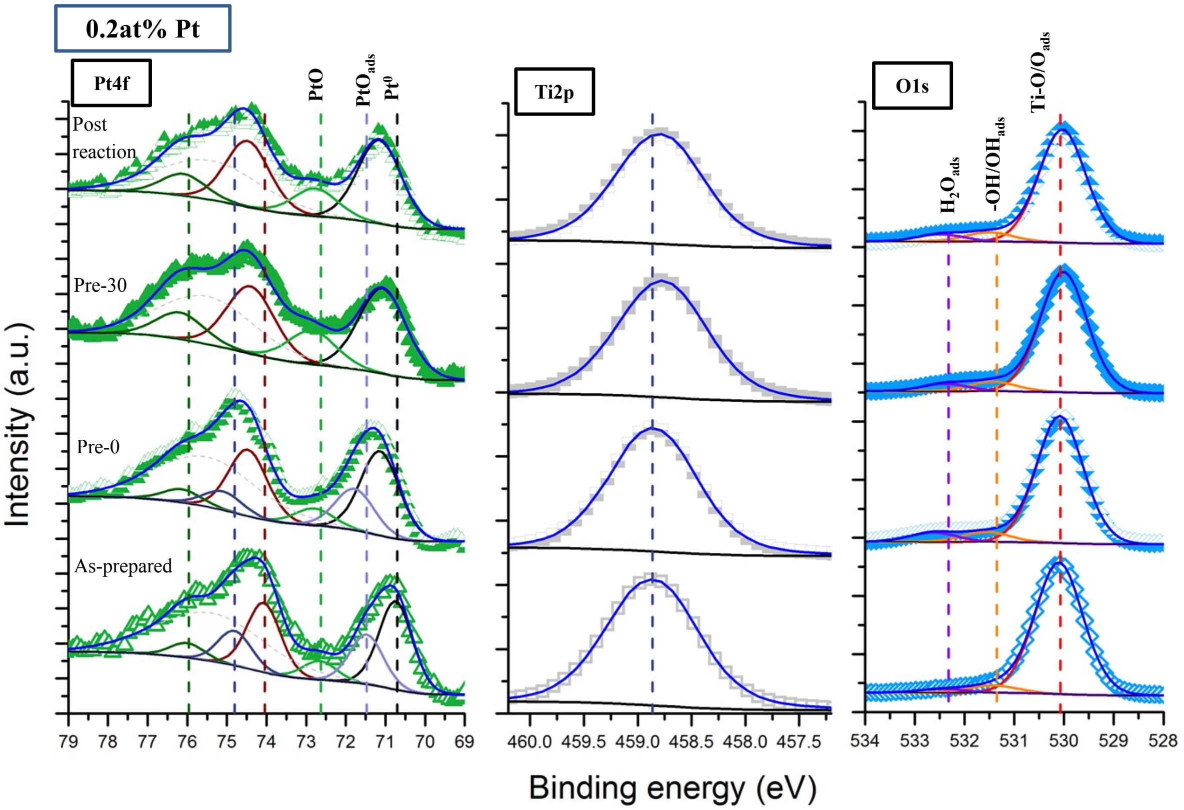

Figure S17. XPS Pt4f, Ti2p, and O1s spectra of 0.2 at% Pt/TiO_2 at the as-prepared state, before UV light pre-treatment (Pre-0), after 30 min UV light pre-treatment (Pre-30), and post-reaction.

REFERENCES

(1) Wong, R. J.; Scott, J.; Low, G. K.-C.; Feng, H.; Du, Y.; Hart, J. N.; Amal, R. *Catal. Sci. Technol.* **2016**.

(2) Zhang, Y.; Pluchery, O.; Caillard, L.; Lamic-Humblot, A.-F.; Casale, S.; Chabal, Y. J.; Salmeron, M. *Nano Lett.* **2015**, *15*, 51–55.

(3) Bus, E.; van Bokhoven, J. A. *J. Phys. Chem. C* **2007**, *111*, 9761–9768.